

Improved Wave Drag Predictions Using Modified Linear Theory

Robert T. Stancil*
Vought Corporation, Dallas, Texas

The combined effect of two simple modifications to supersonic linear theory has resulted in significantly improved local pressure and drag predictions. The two modifications are 1) use of the exact boundary condition, and 2) use of the local (perturbed) Mach number to calculate $\beta = \sqrt{M^2 - 1}$. Comparisons with exact theory and test data are shown for two-dimensional ramps, aircraft wings, cones, and other axisymmetric bodies. The modified linear theory agrees with the exact theory and test data much better than ordinary linear theory, particularly for the larger slopes and nonslender cases. Also, the modified theory predicts only finite perturbation velocities and eliminates the unrealistic peak drags at sonic edge conditions predicted by ordinary linear theory and slender-body theory. Computational aspects are discussed. Because of the good correlations obtained for both planar and axisymmetric cases, the method is now being developed for complete aircraft configuration calculations.

Introduction

THE limitations of supersonic linearized theory in predicting pressure distributions and drag have been well known for many years. Slender-body theory and area rule are special cases of linearized theory. The largest discrepancies occur when the sweep angle is nearly equal to the Mach angle ($\cos^{-1} 1/M$). While linear theory does remarkably well in predicting lift and pitching moment, it does not do as well in predicting drag. Inaccurate prediction results because drag is the integral of pressure times slope, and the largest errors in predicted pressure are likely to occur where the local slopes are largest. Van Dyke's second-order method gives much improved accuracy relative to slender-body or linear theory results for two-dimensional flow, either planar or axisymmetric, but a method for extending it to three dimensions has not been found. For aircraft configurations, there has been no analytical method for predicting drag more accurately than area rule, short of the very complex "exact" solutions such as method of characteristics, time-dependent equations of motion, or relaxation techniques. These exact methods require large amounts of computer time and are often sensitive to input data smoothness, choice of arbitrary parameters, etc. In other words, the techniques are not ideal for application to preliminary design, where many answers are required quickly. Preliminary design requires a method which approximates linear theory in complexity and approaches the exact solutions in accuracy. The modified linear theory technique described herein provides such a method.

Linear Theory Perturbation Relations

Because line distributions of sources and sinks are inadequate for a general three-dimensional solution, all calculations described in this paper utilize surface distributions of sources and sinks. The velocity potential equation is

$$\phi(x, y, z) = \frac{-V_0}{\pi} \iint \frac{S(x_1, y_1, z_1) dx_1 ds}{\sqrt{(x-x_1)^2 - \beta^2(y-y_1)^2 - \beta(z-z_1)^2}} \quad (1)$$

Presented at the AIAA 3rd Atmospheric Flight Mechanics Conference, Arlington, Texas, June 7-9, 1976 (not included in Conference Proceedings); submitted Sept. 28, 1977. Copyright © American Institute of Aeronautics and Astronautics, Inc., 1976. All rights reserved.

Index categories: Aerodynamics; Supersonic Flow; Computational Methods.

*Senior Engineer, Flight Technologies. Associate Fellow AIAA.

where S is the source strength, $ds = \sqrt{dy_1^2 + dz_1^2}$ on the surface of the body, and the integral is taken over that portion of the surface included in the Mach forecone from the point x, y, z . Now, under certain nonrestrictive conditions, the perturbation velocity components can be derived to be of the form

$$v_x = \phi_x = \frac{-V_0 S(x, y, z)}{\beta(I - \beta \tan \epsilon)} + \frac{I}{\pi} \int \frac{F}{\beta} dx_1 \quad (2)$$

$$v_n = \phi_n = \frac{V_0 S(x, y, z)}{I - \beta \tan \epsilon} + \frac{I}{\pi} \int \frac{G}{\beta} dx_1 \quad (3)$$

$$v_p = \phi_p = \frac{I}{\pi} \int \frac{H}{\beta} dx_1 \quad (4)$$

where ϵ is the local slope, v_n is the perturbation component perpendicular to the freestream and normal to v_p , and v_p is the perturbation component perpendicular to the freestream and parallel to the local surface. The functions F , G , and H are dependent on the value of β , the limits of integration, the geometry of the model, and the functions used to describe the variations of source strength in the y, z directions.

Modifications to Linear Theory

The accuracy of the current method results from the combined effects of two modifications: application of the exact boundary condition, and use of the local (perturbed) value of $\beta = \sqrt{M^2 - 1}$. An iterative solution is required because both modifications are dependent on the perturbed values of local velocities. The exact pressure coefficient equation is also used.

The exact boundary condition (Fig. 1) requires not only the use of the perturbed streamwise velocity component but also the determination of the surface slope (ϵ) in the plane defined by the freestream velocity vector and the normal to local surface. This three-dimensional determination of the slope and the velocity component boundary conditions is necessary even in quasiplanar cases, such as for wings.

The primary effect of the local β (Fig. 2) is on the constant of proportionality, $1/\beta$. The $1/\beta$ factor appears in every term but one on the right side of Eqs. (2-4). Thus, it has a direct effect on each of the perturbation velocities. As the local Mach number approaches 1.0, the value of $1/\beta$ approaches infinity. This is obviously an undesirable result. Therefore, a correlated local Mach or β has been developed based on calculations for two-dimensional ramps and cones. The correlation puts a limit on the maximum value of $1/\beta$ and

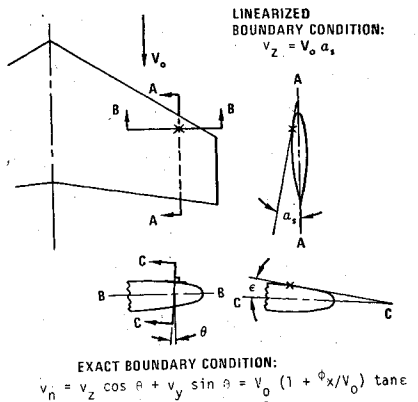


Fig. 1 Modification 1: exact boundary condition.

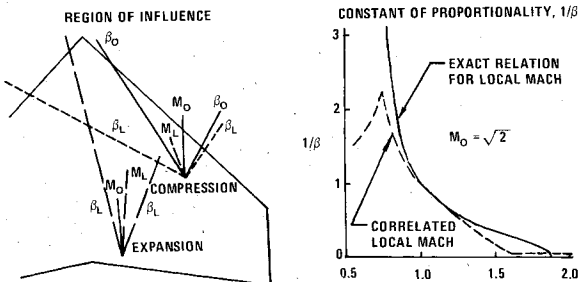
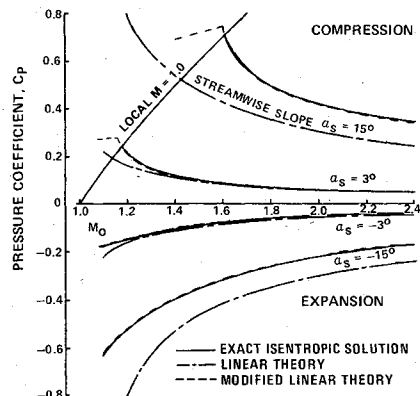
Fig. 2 Modification 2: local β .

Fig. 3 Two-dimensional ramp pressures.

causes the correlated value to approach the limit more slowly than with the exact equation. The effect of local β on the region of influence (characteristic directions) is less pronounced, particularly for two-dimensional cases, either planar or axisymmetric. However, for three-dimensional flow the variations in propagation direction can be important because of the lateral or longitudinal displacement of interference effects. Region of influence effects will be discussed further in the section on computational aspects.

The two modifications have opposite effects. For compressions, the exact tangency condition tends to reduce the magnitude of the perturbations because $(1 + \phi_x/V_0)$ is less than unity, and the required normal velocity v_n is less than with the linearized boundary condition. But the local β in Eqs. (2-4) tends to increase the perturbation values for compressions because, when M is smaller than the freestream value, $1/\beta$ is larger. Conversely, for expansions, $(1 + \phi_x/V_0) > 1$, and the required v_n is larger than the linearized values, but $1/\beta$ is smaller than the freestream value.

Theoretical pressures predicted by the present method are compared with exact theory and linearized theory for unswept ramps (Fig. 3) and 45-deg swept ramps (Fig. 4). The modified

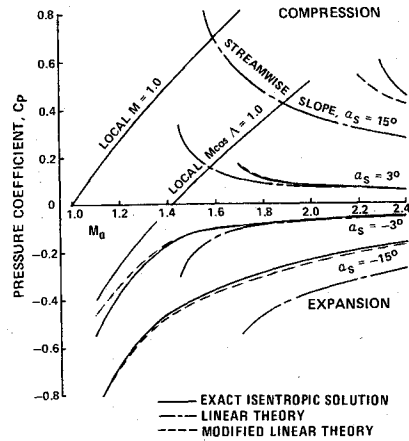


Fig. 4 45-deg sweep ramp pressures.

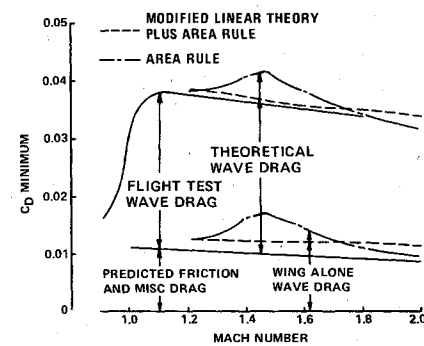


Fig. 5 F-8C wave drag.

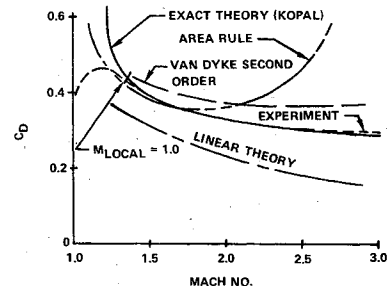


Fig. 6 20-deg cone drag.

linear theory shows greatly improved correlation with exact theory relative to ordinary linear theory for both expansions and compressions. Also, where the linear theory predicts infinite perturbations at sonic edge conditions for the swept ramp in Fig. 4 ($M_0 = \sqrt{2}$), the modified theory on the expansion side shows no tendency toward infinity. Use of the local β eliminates expansion singularities because $1/\beta$ approaches zero with finite positive perturbations. On the compression side, the exact and modified theories cannot be computed at $M_0 = \sqrt{2}$ for this two-dimensional case because the flow could not actually remain two-dimensional. However, it can be seen that the modified theory will not predict infinite perturbations here either, because as $\phi_x/V_0 \rightarrow -1$, exact boundary conditions cause v_n and the source strength to approach zero. Thus, an equilibrium must be reached with the value of ϕ_x/V_0 between 0 and -1.0 .

Numerical Results and Comparisons

Wings

The first application of the modified linear theory method was to the calculation of thickness drag for planar surfaces (wings and tails). Only the exposed panels are considered, and when the wing or tail butts up against the fuselage a reflection plane is assumed at the wing/body intersection.

Figure 5 shows the dramatic improvement in correlation of prediction with flight-test wave drag on the F-8C when the

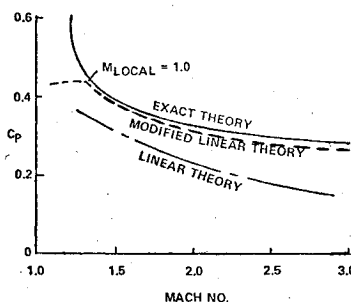


Fig. 7 20-deg cone pressures.

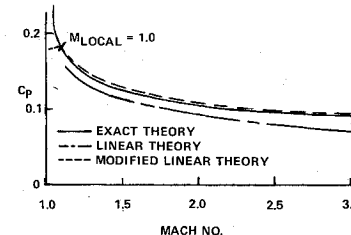


Fig. 8 10-deg cone pressures.

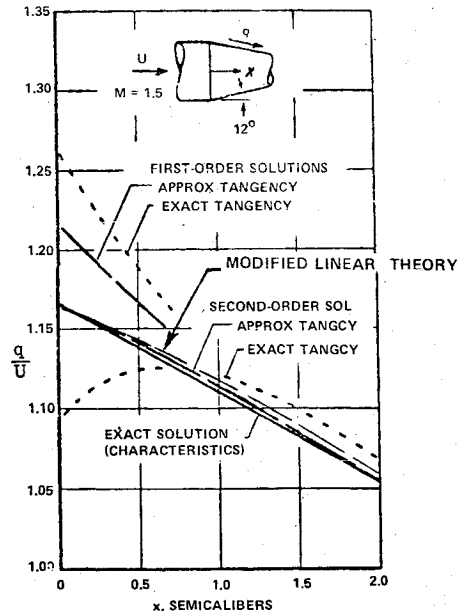


Fig. 9 Conical boattail velocities.

wing and tail wave drags from area rule are replaced by the modified linear theory values. The elimination of the sonic edge drag peak, which tests show does not exist, and the prediction of higher drag than area rule when the leading edge is supersonic are typical of many cases computed by the modified linear theory. The F-8C, with its low-drag canopy and shrouded engine exhaust, has low slopes everywhere except on the wing and tails, and therefore its drag is predicted well once the wing and tail drags are corrected. However, many current configurations have high-visibility canopies, high afterbody slopes, and other components where accurate (nonlinear) calculation of three-dimensional effects is required.

The sonic edge peak drag predicted by area rule is much less of a problem for thinner airfoils or very highly swept wings. But area rule calculations for a 45-deg swept, $t/c = 0.05$ biconvex airfoil case still exhibit a false drag peak (15% high).

Cones

In Fig. 6, experimental data¹ for drag of a 20-deg semivertex angle cone are compared with several theoretical predictions. The exact theory of Kopal agrees with experiment

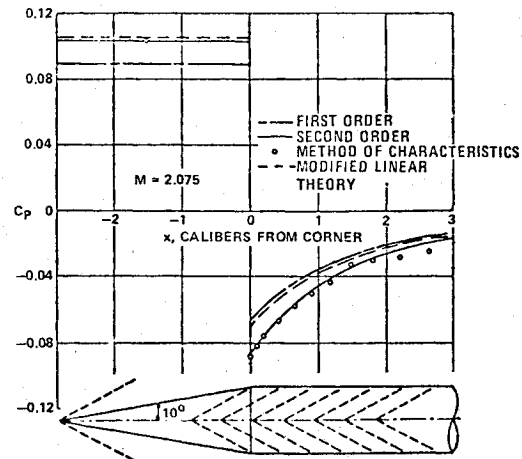


Fig. 10 Cone-cylinder pressures.

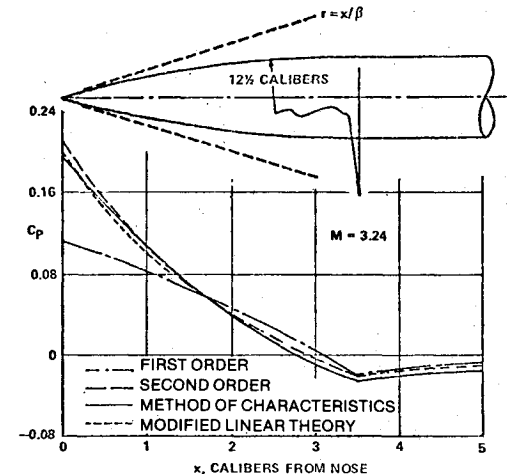


Fig. 11 Ogive-cylinder pressures.

when the flow is supersonic. When the local flow becomes subsonic, the test values of drag level off and finally decrease as the freestream Mach number decreases, but the exact theory values continue to increase. This discrepancy arises because the exact theory assumes conical flow, which is not attained when the local flow becomes subsonic. The area rule predictions agree well with test within the Mach range from 1.2 to 1.9. Below 1.2, where the local flow is subsonic, the area rule prediction continues to increase, and above 1.9, where the Mach angle is approaching tangency to the local slope, the area rule prediction diverges from the data. Linear theory predictions for this case are poorer than the area rule values. Van Dyke's second-order theory overpredicts the drag somewhat. Van Dyke's method will not provide a solution when the local flow becomes subsonic or when β times the local slope is greater than unity.

From Fig. 6, it was seen that the correct (experimental) values of cone pressures or drag were the exact theory values when the local flow is supersonic, with a leveling or falling off as the Mach number is reduced below that for local Mach (M_L) = 1.0. In Fig. 7 for a 20-deg cone and Fig. 8 for a 10-deg cone, the modified linear theory predictions agree very well with the desired values.

General Axisymmetric Bodies

The present method is compared with the method of characteristics and Van Dyke's first- and second-order solutions in Figs. 9-12 for four bodies which Van Dyke used as examples.^{2,3} The modified linear theory predictions agree much better with the characteristics solution than does the

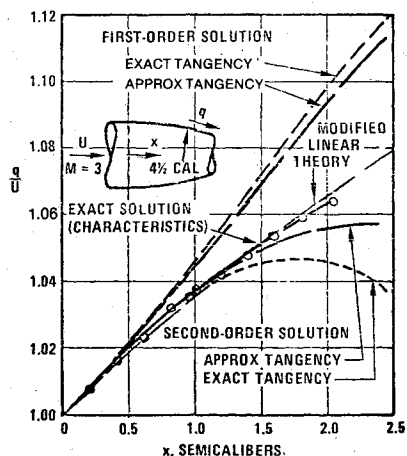
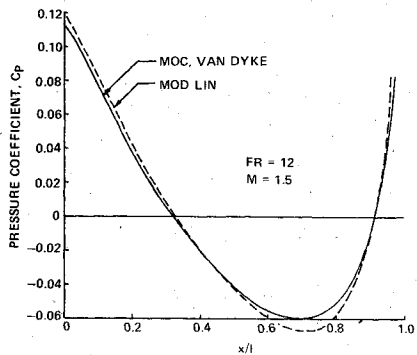
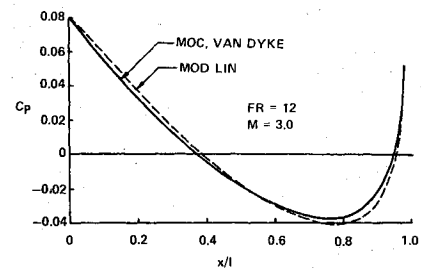


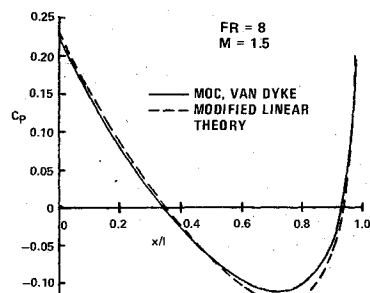
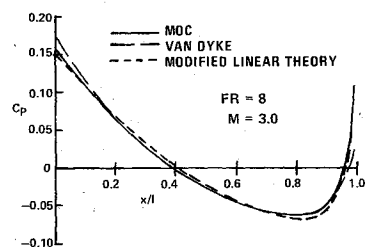
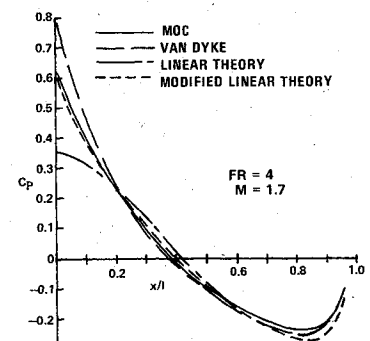
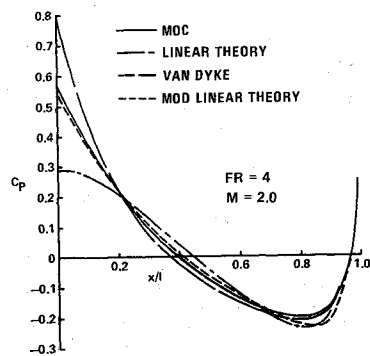
Fig. 12 Circular arc boattail velocities.

Fig. 13 Fineness ratio 12 circular arc body, $M = 1.5$ (MOC = method of characteristics).Fig. 14 Fineness ratio 12 circular arc body, $M = 3.0$ (MOC = method of characteristics).

linear solution. Compared to the Van Dyke second-order solution, the modified linear results are not quite as accurate in Figs. 9 and 10 and are equal to or better than in Figs. 11 and 12.

In Figs. 13-19, predictions by the method of characteristics,⁴ Van Dyke, and modified linear theory are compared for circular arc bodies of revolution at three values of fineness ratio. The modified linear theory values generally agree well with the characteristics solutions, except that the maximum expansion pressures are overpredicted by about 10%. For the higher fineness ratios (8 and 12) in Figs. 13-16, the Van Dyke second-order results agree very well with the exact solution, but for fineness ratio 4 in Figs. 17-19, the Van Dyke results are not as good as the modified linear theory, particularly on the forebody, and at Mach 3 no solution is possible with the Van Dyke method because the product of freestream β and local slope is greater than unity. The present method achieves a solution because local β times local slope is less than unity.

In summary, for the circular arc bodies of revolution, the modified linear theory is not as accurate as Van Dyke's

Fig. 15 Fineness ratio 8 circular arc body, $M = 1.5$.Fig. 16 Fineness ratio 8 circular arc body, $M = 3.0$.Fig. 17 Fineness ratio 4 circular arc body, $M = 1.7$.Fig. 18 Fineness ratio 4 circular arc body, $M = 2.0$.

second-order method for slender bodies but is more accurate and/or provides a solution where the Van Dyke method fails for blunter bodies. Also, a large part of the inaccuracy for slender bodies is due to a computational technique (as opposed to the basic modified theory method) which will be discussed further under computational aspects.

Computational Aspects

Beta Correlation

The correlated relationship for β was empirically determined to give exact agreement between the modified linear theory predictions and the exact isentropic solution for two-dimensional ramps with local supersonic flow. Test data on cones was used to establish the variation of β when the local flow is subsonic. The maximum value of $1/\beta$ is limited to about 2.5, which corresponds to a Mach number of 1.08. For

Fig. 19 Fineness ratio 4 circular arc body, $M = 3.0$.

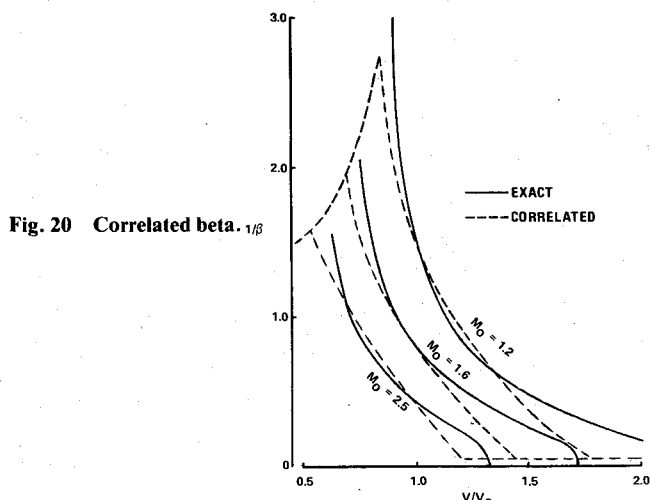
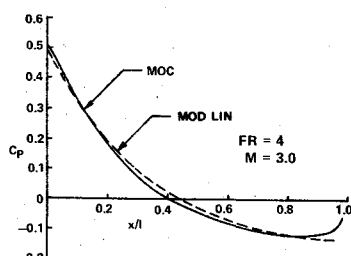
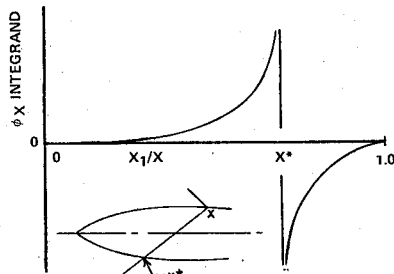


Fig. 21 Typical integrand.



several freestream Mach numbers, the correlated and exact $1/\beta$ functions are compared in Fig. 20.

Characteristics Tracing vs See-Through

A typical plot of the integrand in Eq. (2) is shown in Fig. 21. The singularity at x^* is first order (i.e., of the form $1/x$) and thus produces an infinite result for integration from one side to the singularity, but the integrand is equal and opposite at $x_1 = x^* + e$ and $x_2 = x^* - e$. Therefore, the result of the total integration is finite if the source strength is continuous. But, if the body has a slope discontinuity, the source strength is discontinuous, and at a point located behind the corner such that x^* is equal to the x of the corner, the perturbation velocities are theoretically infinite.

This is a rather absurd result to get an infinite perturbation from an area which actually cannot influence the point under consideration at all. If characteristic tracing is performed, the point at $x_1 = x^*$ and $\theta = \pi$ will be outside of the influencing region. If the θ integration is taken to the characteristic line, the integrand is finite everywhere.

The usual linear theory (or see-through) integration boundaries are compared with the actual characteristic boundaries in Fig. 22. For point A, the difference in the influencing region is not great, but use of the characteristic boundaries does avoid the singularity problem discussed previously. At point B, the see-through method is obviously unusable with surface sources because the Mach forecone

Fig. 22 Alternate influencing regions.

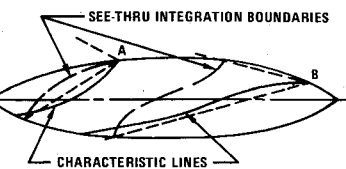


Fig. 23 See-through variation, $FR = 12$ circular arc body, $M = 1.5$.

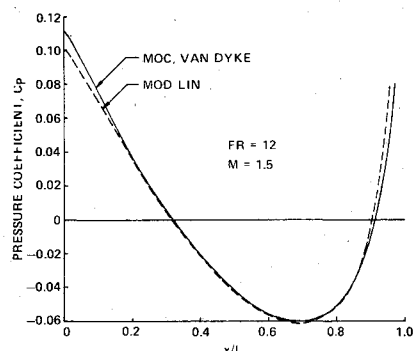
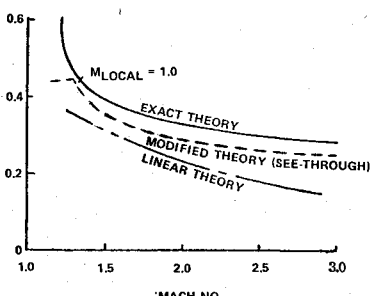


Fig. 24 See-through variation, 20-deg cone.



does not include the surface anywhere near point B. This condition occurs when $\beta(dr/dx) < -1$, and while extreme, it does occur on the fineness ratio 4 body at Mach 2.0 and 3.0 (Figs. 18 and 19), where the characteristic tracing method gave good results. All calculations shown so far have utilized the characteristic tracing method, with an x stretching as required to keep the hyperbolic radius positive.

Use of the characteristic tracing method is the cause of the slight overprediction of expansion pressures mentioned previously, as shown by the improved correlation in Fig. 23 for the afterbody of the fineness ratio 12 body at Mach 1.5 with see-through relative to the previous result in Fig. 13. However, for nose cones, the see-through method underpredicts, as shown in Fig. 24. This difference is as large as the expansion overprediction of the characteristic tracing method and becomes a larger percentage as the cone angle is increased. It is concluded that, except for smooth, quite slender bodies, the characteristic tracing method is superior to the see-through because of 1) the elimination of the infinite perturbation from a slope discontinuity, 2) the capability to calculate accurately when $\beta(dr/dx) < -1$, and 3) the numerical accuracy on moderate- and high-angle cones. These benefits outweigh the overprediction of maximum expansion pressures which occurred on the circular arc bodies.

Continuing Development

An effort is currently underway to program the modified linear theory method for complete aircraft configuration calculations. It is expected that this program will provide a capability for much more accurate and reliable supersonic drag prediction than is the case for current techniques. In particular, prediction of incremental effects, which are important in preliminary design analyses and tradeoff studies, will be much more reliable. The method does not "blow up" when the Mach angle approaches or exceeds tangency to the

local slope. When the local flow becomes subsonic, it does not blow up, and if subsonic flow only happens at the nose of a body, the results are probably accurate; in any event, the local Mach number can be printed and examined by the engineer to assess validity of results.

Conclusions

Two simple modifications to supersonic linear theory result in significantly improved local pressure and drag predictions for both planar and axisymmetric cases. The modified linear theory appears comparable in accuracy to Van Dyke's second-order theory. The modified linear theory method eliminates or greatly relieves limitations of the area rule and ordinary linear theory associated with infinite perturbation velocities, "sonic-edge" conditions, the small-perturbation assumption,

sensitivity of drags to cutting plane location, and lack of local pressures for insight.

References

- ¹Geudtner, W.J., Jr., "Sharp and Blunted Cone Force Coefficients and Centers of Pressure from Wind Tunnel Tests at Mach Numbers from 0.5 to 4.06," Convair, San Diego, Calif., Rept. ZA-7-017, June 1955.
- ²Van Dyke, M.D., "Practical Calculation of Second-Order Supersonic Flow Past Nonlifting Bodies of Revolution," NACA TN 2744, July 1952.
- ³Van Dyke, M.D., "A Study of Second-Order Supersonic Flow Theory," NACA Rept. 1081, 1952.
- ⁴Sawyer, W., private communication. NASA Langley Research Center, 1976.

From the AIAA Progress in Astronautics and Aeronautics Series..

EXPERIMENTAL DIAGNOSTICS IN COMBUSTION OF SOLIDS—v. 63

Edited by Thomas L. Boggs, Naval Weapons Center, and Ben T. Zinn, Georgia Institute of Technology

The present volume was prepared as a sequel to Volume 53, *Experimental Diagnostics in Gas Phase Combustion Systems*, published in 1977. Its objective is similar to that of the gas phase combustion volume, namely, to assemble in one place a set of advanced expository treatments of the newest diagnostic methods that have emerged in recent years in experimental combustion research in heterogeneous systems and to analyze both the potentials and the shortcomings in ways that would suggest directions for future development. The emphasis in the first volume was on homogenous gas phase systems, usually the subject of idealized laboratory researches; the emphasis in the present volume is on heterogeneous two- or more-phase systems typical of those encountered in practical combustors.

As remarked in the 1977 volume, the particular diagnostic methods selected for presentation were largely undeveloped a decade ago. However, these more powerful methods now make possible a deeper and much more detailed understanding of the complex processes in combustion than we had thought feasible at that time.

Like the previous one, this volume was planned as a means to disseminate the techniques hitherto known only to specialists to the much broader community of research scientists and development engineers in the combustion field. We believe that the articles and the selected references to the current literature contained in the articles will prove useful and stimulating.

339 pp., 6 x 9 illus., including one four-color plate, \$20.00 Mem., \$35.00 List

TO ORDER WRITE: Publications Dept., AIAA, 1290 Avenue of the Americas, New York, N.Y. 10019